

Mineral phases of green liquor dregs, slaker grits, lime mud and wood ash of a Kraft pulp and paper mill

Fernanda Machado Martins^a, Joaniel Munhoz Martins^b, Luiz Carlos Ferracin^c,
Carlos Jorge da Cunha^{a,*}

^a *Laboratório de Química Mineral Aplicada, Departamento de Química-UFPR, Universidade Federal do Paraná (UFPR),
CP 19081, CEP 81531990, Curitiba-PR, Brazil*

^b *Laboratório de Análise de Minerais e Rochas (LAMIR-UFPR), Brazil*

^c *Laboratório Químico da Votorantin Cimentos, Brazil*

Received 2 October 2006; received in revised form 13 January 2007; accepted 15 January 2007

Available online 20 January 2007

Abstract

Four residues generated in a Kraft, pulp and paper plant, were characterized by X-ray fluorescence spectroscopy (XFA), powder X-ray diffraction (XRD), thermogravimetric analysis (TG) and Fourier transform infrared spectroscopy (FTIR). A quantitative phase composition model, that accounts for the observed data and for the physico-chemical conditions of formation, was postulated for each material. Emphasis was given on the identification of the mineral components of each material. The green liquor dregs and the lime mud contain Calcite and Gipsite. The slaker grits contains Calcite, Portlandite, Pirssonite, Larnite and Brucite. The Calcite phase, present in the dregs and in the lime mud, has small amounts of magnesium replacing calcium. The wood ash contains Quartz as the major crystalline mineral phase.

© 2007 Elsevier B.V. All rights reserved.

Keywords: Solid residues; Powder X-ray diffraction (XRD); Fourier transform spectroscopy (FTIR); X-ray fluorescence (XFA); Thermogravimetric analysis (TG)

1. Introduction

Brazil, in 2005, has produced 10.1 million metric tonnes of cellulose (air dried pulp) and 8.6 million metric tonnes of paper. It is the seventh world producer of cellulose, accounting for 4.0% of the world production and is the 11th world producer of paper, accounting for 2.4% of the world production (Bracelpa, 2005) [1]. Paraná State has 52 factories of cellulose and/or paper and accounts for 8.6% of the national production. The national production of residues from cellulose plants, was estimated by the authors, as being 128, 166, 153 and 47 thousand metric tonnes of lime mud, slaker grits, green liquor dregs and wood ash, respectively.

In Brazil most industrial solid residues are landfilled. The “Paraná State Inventory of Industrial Solid Residues, 2002” [2] reveals that landfilling is the main destination for the residues followed by fertirrigation and soil disposition.

The present work aims at the identification and quantification of the mineral phases present in the solid residues generated at a local Kraft pulp and paper plant namely, green liquor dregs, slaker grits, lime mud and wood ash. The techniques used were elemental analysis from X-ray fluorescence (XFA), X-ray powder diffraction (XRD), Fourier transform infrared (FTIR) and thermogravimetric analysis (TG). The present work sets an integrated (XFA, TG, XRD, FTIR) approach to identify and quantify the major mineral phases present in this type of materials, that can be applied to other Kraft pulp and paper plants. A routine phase quantification analysis of materials, made available to process engineers, would certainly improve their ability to control operating conditions, increasing product quality and minimizing material and energy losses. The results should also contribute to convert residues into products with the highest possible market value.

A review of the pertinent literature revealed few articles concerned with the characterization of these types of residues. Most of them focus on the disposition on soil for either agriculture or forestry [3–5]. The leaching of contaminants and nutrients from green liquor dregs is reported in detail [6].

* Corresponding author. Tel.: +55 41 3361 3181; fax: +55 41 3361 3186.
E-mail address: cjdcunha@quimica.ufpr.br (C.J. da Cunha).

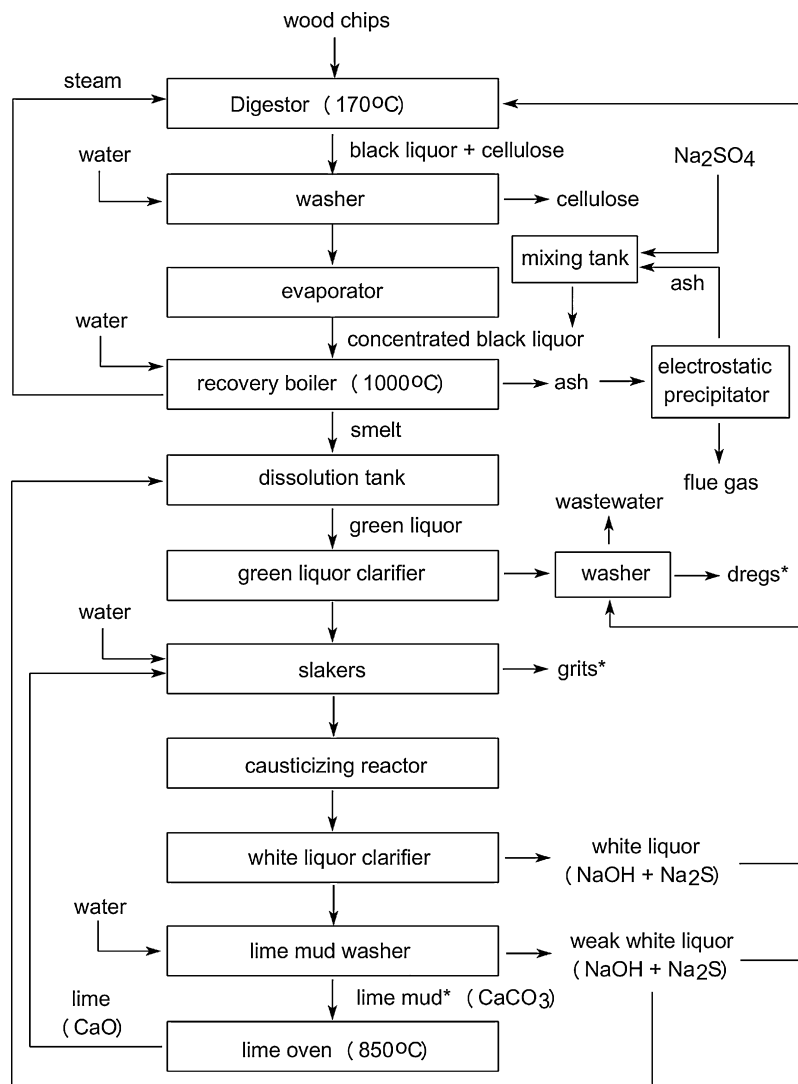


Fig. 1. Flowsheet of the Kraft process under study. The materials sampled are marked with an asterisk. The boiler that generated the wood ash is not shown.

The articles above use elemental analysis and/or speciation to characterize the materials, and do not use TG, XRD and FTIR. Although, a laboratory study, regarding the causticization of sodium carbonate, reports TG/DTA and XRD data [7].

The flowsheet for the Kraft process, of the industry in focus, can be seen in Fig. 1. The materials under study are pinpointed in the flowsheet. Since this process is described in the literature [8], only the aspects relevant to the interpretation of results will be discussed in a proper section.

2. Experimental

2.1. Sampling

Sampling of the four residues was performed according to the Brazilian standard [9]. The green liquor dregs and wood ash were sampled from piles disposed over the ground. The slaker grits and lime mud were sampled right after their generation on

the slakers and lime washer, respectively. The sampled materials are pinpointed in the flowsheet (Fig. 1).

2.2. Sample preparation and analysis

Each sample, of approximately 2 kg of residue (dregs, grits, lime mud, wood ash), was dried at 70 °C for 48 h, ground and divided with a riffle splitter to obtain a 15 g sample. This sample was milled, in a Herzog vibration grinding mill, for 1 min, to get a powder suitable for XFA, XRD, TG and FTIR measurements and for the calcination experiment. The calcination experiment was performed in new porcelain crucibles at 1000 °C for 3 h. The calcined samples were cooled slowly inside a desiccator with silica gel.

The XFA measurements were performed in a PHILIPS, model PW 2400 at LAMIR-UFPR laboratory. The powdered samples were mixed with wax and pressed to form a pellet. The results were interpreted with the software semi-Q PHILIPS and were normalized to 100%. This normalization takes into account

the loss on ignition (LOI) estimated as the total mass loss measured in the TG experiment. The LOI for the wood ash is the one obtained from calcination at 1000 °C for 3 h. The percentage error in the determination of each element concentration with XFA depends on the number of counts (integrated fluorescence intensity). The error increases when the element concentration decreases according to the expression $\%error = 100/(counts)^{1/2}$.

The powder XRD was performed in the dried samples, referred to as “in natura” from now on, and in the calcined samples. The diffractometer used was a Shimadzu, Lab-X model XRD-6000 (radiation Cu K α , $\theta/2\theta$ scans, 40 kV and 30 mA) located at the Chemistry Department-UFPR. The equipment resolution is $\pm 0.01^\circ$. The diffractograms were interpreted with the aid of the data banks of JCPDS [10]; Mincrust [11] and Webmineral [12].

TG data was obtained on a thermal analyser LECO, model TG-601 of the Chemical Laboratory of Votorantim Cimentos. A sample of approximately 1 g was placed in a porcelain crucible and heated, under a nitrogen flux of 4 L min $^{-1}$, at 100 °C until a “dried sample” plateau was reached, then, the sample was heated at a rate of 10 °C min $^{-1}$ up to 1000 °C. The balance precision is ± 0.0001 g and the furnace temperature stability is ± 4 °C.

FTIR spectra were collected on a FTIR BOMEM model MB-100, of the Chemistry Department-UFPR, on KBr pellets, between 4000 and 400 cm $^{-1}$ with a 4 cm $^{-1}$ resolution and 32 scans.

3. Results and discussion

3.1. Characterization of materials

3.1.1. Elemental characterization

Table 1 has the semi-quantitative analysis and interpreted TG mass losses for the samples of dregs, grits, lime mud and wood ash. All elements detected in the samples, including those present in trace amounts, are listed in Table 1. Trace elements, other than those listed in Table 1, may be present in the residues if their concentration is not high enough to generate a significant X-ray fluorescence signal.

A comparison between these values with the few ones reported in the literature reveals that the compositions are largely dependent on the source, probably due to the use of different raw materials and different processing. This variability calls for specific studies, in each processing plant, for a correct characterization.

The elemental compositions of green liquor dregs samples, found in the literature, display sodium contents that vary between 9 and 13%, calcium contents that vary between 27 and 44% and magnesium contents that vary between 0.5 and 3.2. Iron, potassium and manganese are present in small amounts in all reported samples of dregs. Small amounts of chlorine, zinc, silicon, aluminum, sulfur and phosphorus may also be present along with various elements in trace amounts

Table 1
Composition (mass %) of green liquor dregs, lime mud, slaker grits and wood ash

Chemical elements (XFA)	Green liquor dregs	Lime mud	Grits	Wood ash
Ca	32.39	36.02	34.62	0.27
Si	0.80	0.37	3.84	3.21
Al	0.38	0.40	1.72	0.92
Mg	1.41	1.30	0.92	0.13
Fe	1.01	0.37	1.03	0.65
Na	1.16	0.82	6.44	Trace
K	0.15	Trace	0.43	0.27
Ti	Trace	Trace	0.21	0.07
Mn	0.86	0.45	0.36	Trace
Ba	Trace	Trace	Trace	Trace
Sr	n.d.	0.16	0.31	n.d.
P	0.14	0.35	0.47	n.d.
Cl	Trace	Trace	0.14	n.d.
O ^a	18.09	17.85	27.23	15.61
S	0.98	0.54	1.62	0.07
Assigned mass loss (TG)				
H ₂ O (Gipsite)	0.66(1) + 0.22 (2)	0.61(1) + 0.20 (2)		
H ₂ O (Pirssonite)			2.78 (1)	
Other volatiles	8.27 (2) ^b	1.57 (2) ^b		
Organic matter				78.90
H ₂ O (Brucite)			1.28 (2)	
H ₂ O (Portlandite)			2.87 (3)	
CO ₂ (Calcite)	33.2 (3)	39.0 (3)		
CO ₂ (Pirssonite and Calcite)			13.7 (4)	
Total	99.72	100.01	99.97	100.10

The values were normalized from XFA and LOI from TG data. The numbers in parenthesis correspond to the thermal events identified in the DTG curves in Fig. 3. The values, for each residue, are relative to one sample and do not represent averaged values.

^a Oxygen present in the fixed oxides was estimated from estequiometry. It does not account for the oxygen of water and carbon dioxide lost on ignition.

^b Total mass loss of process (2) less the calculated amount of water lost in the process $\text{CaSO}_4 \cdot 0.5\text{H}_2\text{O} \rightarrow \text{CaSO}_4 + 0.5\text{H}_2\text{O}$.

[4,5,13,14]. Nurmesniemi et al. [6] studied a sample of dregs and reported the percentage of major and trace elements that leach from the sample.

The articles reporting an elemental characterization of lime mud [4,5] display calcium contents between 10 and 38%. All other cations, present in lime mud, have a small concentration being sodium, iron, magnesium and manganese the most important ones. Small amounts of other elements such as phosphorus, potassium, chlorine, zinc, sulfur, boron and fluorine are also reported along with a large number of other elements in trace amounts.

The sample of slaker grits studied here has a slightly smaller calcium content, is higher in sodium, sulfur, magnesium, potassium and iron and is lower in manganese, when compared to the only slaker grits composition found in the literature [4].

The wood ash is mainly composed of volatile material being Si the most abundant element detected by XFA. A meaningful comparison of chemical compositions of ashes is very difficult because the tree's composition, that originate the ashes, depends on various factors such as the type of forest species, part of plant combusted (bark, wood, leaves), plant age, type of soil, climate, conditions of combustion [15]. Nevertheless, it can be affirmed that the wood ash residue studied here has not been completely ashed because of its high content of volatiles compared to that of true ashes that display a maximum of 34% volatiles [15]. The wood ash analysed in the present study originates from bark and wood chips unsuitable to be pulped. The pine species used in the plant is *Pinus taeda*.

3.1.2. Mineralogic characterization

The diffractograms of samples “in natura” of wood ash, green liquor dregs, lime mud and slaker grits can be seen in Fig. 2.

The diffractograms of the green liquor dregs and lime mud are very similar and are dominated by a phase of Calcite with small amounts of magnesium replacing calcium. This phase can be best represented as $\text{Ca}_{(1-x)}\text{Mg}_x\text{CO}_3$. Calcites are able to bear small amounts of Mg in their structure [16].

In the slaker grits diffractogram, Calcite (CaCO_3) and Pirssonite ($\text{CaNa}_2(\text{CO}_3)_2 \cdot 2\text{H}_2\text{O}$) are the dominant phases followed by Portlandite ($\text{Ca}(\text{OH})_2$) and Wustite (FeO). The presence of Larnite (Ca_2SiO_4) cannot be ruled out.

The diffractograms of the calcined samples of dregs and lime mud (not shown) reveal the presence of calcium magnesium oxide ($\text{Ca}_{(1-x)}\text{Mg}_x\text{O}$) and Periclase (MgO), as expected from the thermal decomposition of $\text{Ca}_{(1-x)}\text{Mg}_x\text{CO}_3$. The diffractogram of the calcined sample of grits displays diffraction peaks of lime (CaO) and Periclase (MgO), the presence of Larnite cannot be ruled out. The expected Natrite ($\gamma\text{-Na}_2\text{CO}_3$) phase was not identified in the calcined grits sample, instead, sodium oxide was undoubtedly identified. In the diffractograms, of all three calcined samples, listed above, low crystallinity Portlandite ($\text{Ca}(\text{OH})_2$), was also detected being its presence interpreted as due to the highly hygroscopic character of calcium oxide.

The diffractogram of the wood ash, in natura, displayed two broad halos, assigned to amorphous carbonaceous material, sim-

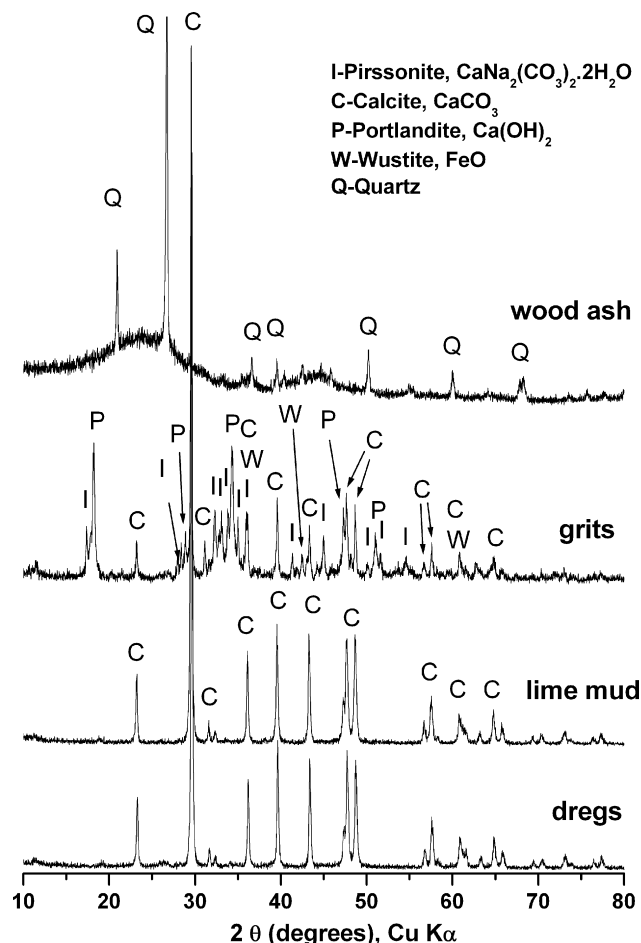


Fig. 2. X-ray powder diffractograms of wood ash, slaker grits, lime mud and green liquor dregs, in natura.

ilar to those observed in coal [17,18]. The only crystalline phase present is Quartz alpha. The diffractogram of the calcined wood ash sample displays Quartz as the major crystalline phase and no amorphous halos are present, in agreement with the disappearance of the carbonaceous material.

No crystalline phases bearing aluminum were identified in the residues analysed here. The aluminum cations are assumed to be present in amorphous phases or dispersed in various minor undetected crystalline phases.

3.1.3. Thermal analysis

The TG/DTG curves for the samples of green liquor dregs, lime mud and slaker grits can be seen in Fig. 3. The assignments of the main (numbered) processes can be seen in Table 1. The dregs and lime mud TG/DTG curves are quite similar displaying partial Gipsite dehydration ($\text{CaSO}_4 \cdot 2\text{H}_2\text{O} \rightarrow \text{CaSO}_4 \cdot 0.5\text{H}_2\text{O} + 1.5\text{H}_2\text{O}$) (process 1), a yet unassigned process that encompasses the dehydration of $\text{CaSO}_4 \cdot 0.5\text{H}_2\text{O}$ (process 2) and loss of CO_2 from Calcite pyrolysis (process 3). It is possible that process 2 involves burning of organic material. The TG/DTG curve for the sample of slaker grits displays Pirssonite dehydration (process 1), Brucite dehydroxylation (process 2), Portlandite dehydroxylation (process 3) and a concomitant CO_2 loss from the pyrolysis of $\text{CaNa}_2(\text{CO}_3)_2$

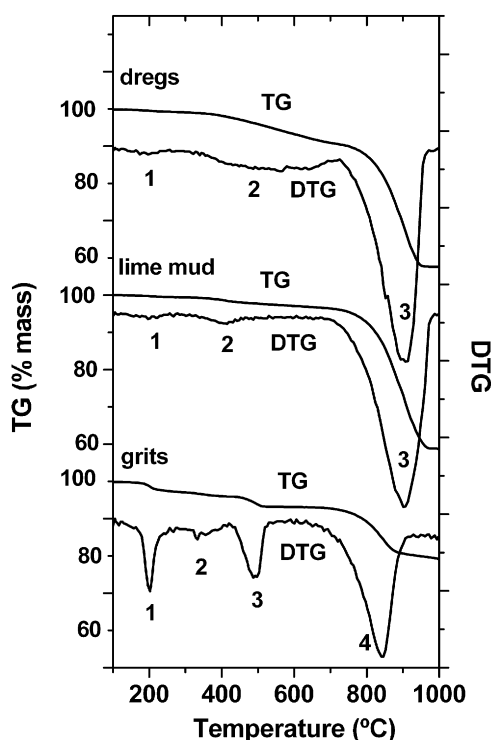


Fig. 3. TG-DTG curves for the samples of green liquor dregs, lime mud and slaker grits under nitrogen flow and a heating rate of $10^{\circ}\text{C min}^{-1}$. The vertical scales of the DTG curves were adjusted for clarity.

and Calcite (process 4). The articles by Zsakó and Hints [7] and by Dheilly and Tundo [19] were instrumental for the interpretation of these thermal decompositions.

The TG/DTG curve for the wood ash sample (not shown) displayed three processes assigned as pyrolysis of organic matter. The overall mass loss is above 76%. The mass loss assigned to this process in Table 1 was taken from the calcination experiment because at the end of the TG experiment, at 1000°C , the mass was still decreasing.

The assignments of TG/DTG processes, given here, are in accordance with XRD phase assignments of in natura and calcined materials. The following phases, detected in the TG experiment, were not detected in the respective diffractograms: Brucite, in the slaker grits and Gipsite, in the green liquor dregs and lime mud.

3.1.4. FTIR spectra

Fig. 4 has the FTIR spectra of wood ash, slaker grits, lime mud and green liquor dregs. All four spectra have bands in the alkane C–H stretch region indicating the presence of organic material. The spectrum of wood ash also has a band in the alkyne C–H stretch region and a band in the C=C stretch region. The spectra of grits, lime mud and dregs have a band in the S–H stretch region. The presence of this band, in the spectra, can indicate the presence of either adsorbed mercaptans or SH^{-} anion. A broad band in the Si–O region is clearly visible in the spectrum of wood ash. Calcite, CaCO_3 , and Calcite with magnesium, $\text{Ca}_{(1-x)}\text{Mg}_x\text{CO}_3$, have some spectral differences that allow their discrimination. The spectrum of grits indicates the presence of

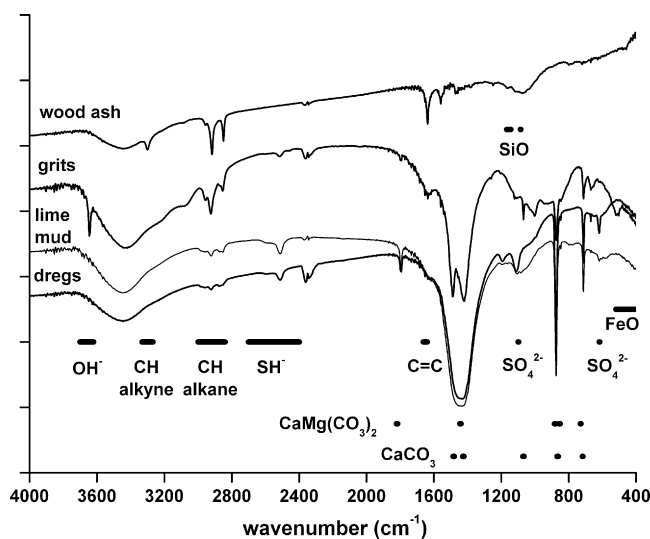


Fig. 4. Infrared spectra of the residues wood ash, slaker grits, lime mud and green liquor dregs, in natura, prepared as KBr pellets. The range of vibrational modes are shown as horizontal bars: SO_4^{2-} and S–H [21]; C–H; C=C and O–H [22]; SiO, $\text{CaMg}(\text{CO}_3)_2$, CaCO_3 and Fe–O [23].

Calcite whereas the spectra of lime mud and dregs indicate the presence of Calcite with magnesium. These assignments are in agreement with those based on XRD interpretation. The presence of the anion sulfate is confirmed in the spectra of lime mud and dregs. This interpretation is in agreement with the assignment of Gipsite ($\text{CaSO}_4 \cdot 2\text{H}_2\text{O}$) in the samples of lime mud and green liquor dregs from TG data (process 1). An intense sharp band, in the slaker grits' spectrum, is assigned to non-hydrogen bonded O–H stretch. This interpretation is in agreement with the assignment of Portlandite ($\text{Ca}(\text{OH})_2$) and Brucite ($\text{Mg}(\text{OH})_2$) based on TG data (processes 2 and 3). The grits spectrum also has a band in the Fe–O stretch region, this is in agreement with the assignment of Wustite in the respective diffractogram. The presence of water in the samples could not be ascertained with these spectra because the KBr used in the pressed pellet is hygroscopic. The mineral phase assignments based on XRD and TG data are in agreement with the interpretations of the infrared spectra given here.

3.1.5. Physico-chemical conditions of residues formation

The physico-chemical conditions under which a residue was formed must be compatible with its elemental and phase compositions and will be considered here.

3.1.5.1. Green liquor dregs. The smelt – composed of molten salts (mainly sulfides, carbonates, sulfates and chlorides of sodium and potassium) – comes out of the recovery boiler, is mixed with water, and dissolves forming the green liquor. The water insoluble material, named green liquor dregs, is removed, washed with weak white liquor and discarded. The presence of Calcite and Gipsite in this residue is in agreement with their water insolubility. The weak white liquor comes from the lime mud washer and adds calcium and magnesium to the dregs composition (Fig. 1).

3.1.5.2. Lime mud. The lime mud is the insoluble material that results from the causticization reaction $\text{Ca}(\text{OH})_2 (\text{aq}) + \text{Na}_2\text{CO}_3 (\text{aq}) \rightarrow \text{CaCO}_3 (\text{s}) + \text{NaOH} (\text{aq})$ and should contain a large amount of Calcite (Fig. 1). The presence of Gipsite in this residue is also possible due to its insolubility.

3.1.5.3. Slaker grits. The lime, produced in the oven, is mixed with water in a series of reactors, named slakers, and dissolved. The slakers also receive the green liquor and the causticization reaction takes place as the lime dissolves. The insoluble material removed from the slakers is named slaker grits (Fig. 1). The assigned Pirssonite phase is in agreement with its insolubility under the slakers' conditions, in fact it is an undesired product [7] since it immobilizes sodium, calcium and carbonate that are important process components. The presence of the partially water soluble Portlandite can also be considered undesirable because it is a reagent in the process of causticization. The presence of Pirssonite and Calcite, in this solid residue means that the main reaction in the lime oven was not complete. Part of the Calcite present in the residue may also have originated from the reaction between $\text{Ca}(\text{OH})_2$ and atmospheric CO_2 . The presence of Brucite is also possible due to its insolubility in aqueous alkaline medium. The Larnite, Ca_2SiO_4 , is believed to have originated from the oven refractory.

3.1.5.4. Wood ash. The wood ash, is produced in a vertical, utility water tube boiler that burns refused wood chips, bark and wood fines. The boiler generates 58 tonnes/h of steam, and is not shown in Fig. 1. The silica identified in this residue is part of the wood composition and the major amorphous organic phase is unburnt biological material derived from cellulose and lignin.

3.1.6. Mineral phase quantification

Taking into account all qualitative and quantitative data collected, a major phase composition model was established for each material (Table 2). The percentages of some phases were estimated from TG data and/or from XFA data. If the mass vari-

ation for a thermal event can be precisely measured from TG data, meaning that it has well-defined plateaus before and after the event, the TG data are highly reliable. Due to the nature of the XFA measurements the smaller the concentration of a given element, the higher the error in its quantification. Despite these limitations, the estimates based on TG and XFA agree well. If a more precise, but far more expensive, quantification is needed, atomic emission spectroscopy (AES) could be used. Phase quantification can also be made from numerical manipulation of XRD data if suitable standards are available. For a better quantification of the MgCO_3 and CaCO_3 contents, in the $\text{Ca}_{1-x}\text{Mg}_x\text{CO}_3$ bearing samples, a TG experiment in CO_2 atmosphere could be run with a slow heating rate [20].

The following specific assumptions were made for the estimations in Table 2.

3.1.6.1. Green liquor dregs and lime mud. The amount of $\text{Ca}_{1-x}\text{Mg}_x\text{CO}_3$ was estimated from the TG CO_2 loss on the pyrolysis and from the XFA amount of Ca and Mg. The value of x was estimated from the XFA amounts of Ca and Mg. The amount of $\text{CaSO}_4 \cdot 2\text{H}_2\text{O}$ was estimated from the corresponding TG H_2O loss on the dehydration and from the XFA amount of S. The unassigned volatiles were evaluated subtracting the estimated (TG and XFA) amounts of CO_2 and H_2O lost from the pyrolysis of Calcite and Gipsite, respectively, from the total volatiles, determined in the TG experiment. The unassigned fixes were evaluated subtracting the estimated (TG and XFA) amounts of CaO, MgO and CaSO_4 from the total fixes, determined in the TG experiment. The unassigned volatiles XFA estimation for the lime mud is negative probably because the XFA Calcite content is overestimated.

3.1.6.2. Slaker grits. The amount of $\text{CaNa}_2(\text{CO}_3)_2 \cdot 2\text{H}_2\text{O}$ was estimated from the TG H_2O loss on dehydration and from the XFA Na content. The large discrepancy between both estimates has not yet been figured out but may be related to the presence of a refractory glassy phase with sodium. The authors

Table 2

Major phase quantification (% mass) for the residues green liquor dregs, lime mud and slaker grits

Phases	Green liquor dregs		Lime mud		Slaker grits	
	TG	XFA	TG	XFA	TG	XFA
$\text{Ca}_{1-x}\text{Mg}_x\text{CO}_3$	75.6	87.4 ($x=0.07$)	88.7	92.5 ($x=0.06$)	23.5 ^a	14.8 ^a ($x=0$)
$\text{CaSO}_4 \cdot 2\text{H}_2\text{O}$	4.3	5.3	3.9	2.7		
$\text{CaNa}_2(\text{CO}_3)_2 \cdot 2\text{H}_2\text{O}$					18.6	33.9
$\text{Ca}(\text{OH})_2$					11.8	11.8 ^b
$\text{Mg}(\text{OH})_2$					4.1	2.2
Ca_2SiO_4					28.4	28.6
Unassigned volatiles ^c	8.3	2.8 ^a	1.6	-1.1 ^a	0.00	0.02
Unassigned fixes	12.8 ^d	6.5 ^d	3.2 ^d	6.7 ^d	13.5 ^e	7.9 ^e
Total	100.9	102.0	100.8	101.5	99.9	101.7

Data on TG and XFA columns were estimated solely from TG and XFA data, respectively, except where stated otherwise.

^a From a combination of TG and XFA data.

^b From TG data.

^c Except H_2O lost by Gipsite, Pirssonite, Portlandite and/or Brucite and CO_2 lost by Calcite and/or Pirssonite.

^d Except CaO, MgO and CaSO_4 .

^e Except CaO, MgO, Na_2CO_3 and Ca_2SiO_4 .

believe the estimations given in the TG column to be more robust than those in the XFA column. The amount of $\text{Ca}(\text{OH})_2$ was estimated from the TG H_2O loss on the dehydroxylation. Since there is no estimation for this phase from XFA data, this figure is repeated in the corresponding cell in Table 2. The amount of CaCO_3 was estimated from the difference, between the moles of CO_2 lost on the pyrolysis of the carbonates and the moles of $\text{CaNa}_2(\text{CO}_3)_2 \cdot 2\text{H}_2\text{O}$. The amount of Ca_2SiO_4 , placed in the TG column in Table 2, was estimated from the molar difference between the total XFA Ca content and the sum of $\text{CaNa}_2(\text{CO}_3)_2 \cdot 2\text{H}_2\text{O}$, CaCO_3 and $\text{Ca}(\text{OH})_2$. The amount of Ca_2SiO_4 , placed in the column XFA in Table 2, was estimated from the XFA Si amount. The TG and XFA Ca_2SiO_4 estimations are almost identical. Despite the fact that Larnite could not be unambiguously assigned in the slaker grits diffractograms of neither in natura nor calcined samples, it is quite reasonable to believe it is present due to the quantitative phase assignment just given and from all slaker grits data seen collectively. The amount of $\text{Mg}(\text{OH})_2$ was estimated from the TG H_2O loss on the dehydroxylation and from the XFA amount of Mg. The unassigned volatiles were evaluated subtracting the estimated (TG and XFA) amounts of CO_2 and H_2O lost from the pyrolysis of Calcite, Pirssonite, Brucite and Portlandite, from the total volatiles, determined in the TG experiment. The unassigned fixes were evaluated subtracting the estimated (TG and XFA) amount of CaO, MgO, Na_2CO_3 and Ca_2SiO_4 from the total fix material, as measured in the TG experiment.

For the residues lime mud, green liquor dregs and slaker grits the unassigned volatiles may comprise H_2O lost from dehydroxylation of hydroxides and or hydrated oxides of minor cations (Table 1) and burning of organic matter, detected in the respective FTIR spectra. The unassigned fixes may comprise the oxides of the minor cations (Table 1).

3.1.6.3. Wood ash. The amount of SiO_2 , 6.8%, was estimated from the XFA Si content and the amount of organic matter, 78.8%, was estimated from the total mass loss on ignition experiment. The amount of unassigned fixes, 14.4%, was evaluated subtracting the estimated amount of SiO_2 from the total amount of fixes determined in the mass loss on ignition experiment.

4. Conclusion

Four residues generated in a Kraft pulp and paper industry, green liquor dregs, lime mud, slaker grits and wood ash, were analysed by FTIR, XRD, XFA and TG and the major phases present in each were identified and quantified based on an integrated approach that included an evaluation of the physico-chemical conditions of each residue formation. The green liquor dregs and the lime mud contain Calcite ($\text{Ca}_{1-x}\text{Mg}_x\text{CO}_3$) and Gipsite ($\text{CaSO}_4 \cdot 2\text{H}_2\text{O}$). The Calcite phase has small amounts of magnesium replacing calcium and the evidences for this assignment come from the XRD and FTIR data. The Gipsite phase, interpreted as being present in small amounts, was not detected in the respective XRD diffractograms but evidences for its presence come from XFA, TG

and FTIR data. The slaker grits contains Calcite (CaCO_3), Portlandite ($\text{Ca}(\text{OH})_2$), Pirssonite ($\text{CaNa}_2(\text{CO}_3)_2 \cdot 2\text{H}_2\text{O}$), Larnite (Ca_2SiO_4) and Brucite ($\text{Mg}(\text{OH})_2$). The former three phases were identified in the XRD diffractogram. The Larnite phase could not be unambiguously identified solely based on XRD data, its presence was revealed from the overall interpretation of all collected data. The presence of Brucite was inferred from TG data and from the presence of Periclase in the XRD diffractogram of the calcined material. The wood ash is mainly composed of organic matter and contains alpha Quartz as the major crystalline mineral phase. The authors hope to have demonstrated the utility of the integrated approach, presented here, to a residue's characterization. The results should aid the industry to find uses for these materials so that they become products instead of residues.

Acknowledgements

The authors would like to acknowledge the following persons and institutions for their intellectual and/or material help: LAMIR-UFPR, Dr. José Manoel dos Reis, Luciane Lemos do Prado, Rodrigo Secchi, Elisiane Roper Pescini, Francielen Pereira da Silva and Carlos Lara Ribeiro; Votorantim-Cimentos, Luciana Bianco and Ana Carolina Luchesi; Chemistry Department-UFPR, Dr. Fernando Wypych, Dr. Sueli Drechsel, Dr. Luiz Pereira Ramos, and Dr. Aldo Zarbin; Cocelpa, Luis F. Gaioto, Mauro Cardoso and Julia de Araujo Basso; Ripasa, Danyella Oliveira Perissotto.

References

- [1] <http://www.bracelapa.org.br>.
- [2] Inventário Estadual de Resíduos Sólidos do Estado do Paraná-IRSEP, Relatório Final para Divulgação-Diagnóstico, 2002.
- [3] A.F.J. Bellote, H.D. Silva, C.A. Ferreira, G.C. Andrade, Resíduos da Indústria de Celulose em Plantios Florestais, Boletim de Pesquisa Florestal, Colombo 37 (1998) 99–106.
- [4] A. Liard, R. Lessard, J. Leclerc, L. Desilets, Product from residue: standard setting for alkaline mill residues in Quebec, Pulp Pap.-Can. 100 (5) (1999) 27–29.
- [5] M. Jordan, M.A. Sánchez, L. Padilla, R. Cespedes, M. Osses, B. Gonzalez, Kraft mill residues effects on monterey pine growth and soil microbial activity, J. Environ. Qual. 31 (2002) 1004–1009.
- [6] H. Nurmesniemi, R.I. Poykio, P. Peramaki, T. Kuokkanen, The use of a sequential leaching procedure for heavy metal fractionation in green liquor dregs from a causticizing process at a pulp mill, Chemosphere 61 (2005) 1475–1484.
- [7] J. Zsakó, M. Hints, Use of thermal analysis in the study of sodium carbonate causticization by means of dolomitic lime, J. Therm. Anal. 53 (1998) 323–331.
- [8] J. Gullichsen, C.J. Fogelholm (Eds.), Chemical Pulping, J. Gullichsen, H. Paulapuro (Eds.), Papermaking Science and Technology, vol. 6, Fapet Oy., Jyväskylä, 2000, p. 497s.
- [9] Associação Brasileira de Normas Técnicas, NBR 10.007: Resíduos Sólidos-Amostragem, Rio de Janeiro, 2004.
- [10] JCPDS-ICDD, International Center for Diffraction Data, 2001.
- [11] <http://database.iem.ac.ru/mincryst/index.php>.
- [12] <http://www.webmineral.com>.
- [13] A.B. Landim, Reciclagem de Resíduos Sólidos-Parte I: Adição de Dregs ao Efluente do Branqueamento Ácido, O Papel. (1995) 32–36.
- [14] J.S. Delcolli, H.A. Oliveira, G.A. Oliveira, S. Toffoli, A Influência do Resíduo Dregs da Fabricação de Papel na Produção de Argila

- Expandida, Anais do Congresso Brasileiro de Cerâmica, vol. 46, São Paulo, 2002.
- [15] S. Liodakis, G. Katsigiannis, G. Kakali, Ash properties of some dominant Greek forest species, *Thermochim. Acta* 437 (2005) 158–167.
- [16] C. Klein, A.S. Hurlbut Jr., Calcite group, in: *Manual of Mineralogy*, 21st ed., John Wiley, New York, 1999, p. 406.
- [17] S. Dai, D. Lic, D. Rena, Y. Tanga, L. Shaoa, H. Songa, Geochemistry of the late Permian No. 30 coal seam, Zhijin Coalfield of Southwest China: influence of a siliceous low-temperature hydrothermal fluid, *Appl. Geochem.* 19 (2004) 1315–1330.
- [18] J. Nover, J.B. Stoll, J.V.D. Gonna, Promotion of graphite formation by tectonic stress—a laboratory experiment, *Geophys. J. Int.* 160 (2005) 1059–1067.
- [19] R.M. Dheilily, J. Tudo, Contribution à l'étude de la gaylussite: $\text{Na}_2\text{Ca}(\text{CO}_3)_2 \cdot 5\text{H}_2\text{O}$, *C.R. Acad. Sci. Paris* 325 (b) (1996) 407–414.
- [20] C. Dagounaki, K. Chrissafis, A. Kassoli-Fournaraki, A. Tsirambides, C. Sikalidis, K.M. Paraskevopoulos, Thermal characterization of carbonate rocks, Kozani area, North-western Macedonia, Greece, *J. Therm. Anal. Calorim.* 78 (2004).
- [21] K. Nakamoto, *Infrared and Raman Spectra of Inorganic and Coordination Compounds*, third ed., John Wiley & Sons, New York, 1970.
- [22] R.M. Silverstein, in: S.A., *Identificação Espectroscópica de Compostos Orgânicos*, Editora Guanabara Dois, Rio de Janeiro, 1979.
- [23] M.J. Wilson, *Clay Mineralogy: Spectroscopic and Chemical Determinative Methods*, first ed., Chapman & Hall, 1994.